The Astrophysical Journal, 577:668–679, 2002 October 1
© 2002. The American Astronomical Society. All rights reserved. Printed in U.S.A.

YOUNG STELLAR NUCLEI IN LENTICULAR GALAXIES: NGC 5574 AND NGC 7457[1]

O. K. Sil'chenko[2]
Sternberg Astronomical Institute, Universitetsky Pr. 13, Moscow State University, Moscow 119992, Russia; and Isaac Newton Institute of Chile, Moscow Branch, Russia; olga@sai.msu.su

V. L. Afanasiev
Special Astrophysical Observatory, Russian Academy of Science, St. Zelenchukskaya, Karachi-Cherkesia, Nizhnij Arkhyz 369167, Russia; vafan@sao.ru

and

V. H. Chavushyan and J. R. Valdes
Instituto Nacional de Astrofísica, Optica y Electrónica, A.P. 51 y 216, C.P. 72000, Puebla, Puebla 72840, Mexico; vahram@inaoep.mx, jvaldes@inaoep.mx
Received 2002 April 29; accepted 2002 June 10

ABSTRACT

The stellar population properties in the centers of NGC 5574 and NGC 7457 (two lenticular galaxies previously shown to have radially homogeneous blue optical-band colors) are studied by means of integral-field spectroscopy. The compact nuclei of the galaxies appear to be chemically distinct: in NGC 5574 the nucleus is distinguished by a higher than solar iron-to-magnesium ratio, and in NGC 7457 a drop of mean stellar metallicity by a factor of 2 exists between the nucleus and the bulge. Both galaxies demonstrate a rather young mean luminosity-weighted age of the stellar populations in the bulges, not older than 5–7 Gyr; however, the chemically distinct nuclei are still younger, 2–2.5 Gyr old. The kinematics of the stars in the center of NGC 5574 are probably affected by the influence of its global bar. The compact core of NGC 7457, with a radius of about 1″.5, shows a visible counterrotation; a combined analysis of the photometric and kinematical two-dimensional maps allows us to conclude that the core rotates axisymmetrically, but its rotation plane is inclined to the main symmetry plane of the galaxy. The stellar velocity dispersion in the centers of both galaxies is anomalously low: 60–80 km s^{-1}.

Subject headings: galaxies: evolution — galaxies: individual (NGC 5574, NGC 7457) — galaxies: kinematics and dynamics — galaxies: nuclei — galaxies: structure

1. INTRODUCTION

A common view is that S0 galaxies are similar to ellipticals with respect to their stellar populations, with both types of galaxies possessing homogeneously old, metal-rich stars. This opinion is mostly due to the fact that the mean integrated colors of S0 and E galaxies are the same (Buta & Williams 1995). Therefore, when we undertook a spectral survey of the central parts of 100 nearby galaxies some years ago (Sil'chenko & Shapovalova 1989; Sil'chenko 1990) and found that half of all lenticulars in our sample demonstrated strong Balmer absorption lines in their spectra, similar to early-type spirals rather than to ellipticals, this finding was unexpected to us. Applying stellar population synthesis and also comparing the data with Galactic globular cluster spectra, we have shown that the mean luminosity-weighted stellar ages in the centers of half of the nearby S0s observed by us are really less than 5 Gyr (Sil'chenko 1993). Later, we began to separate the stellar populations of the unresolved nuclei from those of the surrounding bulges because their properties (and so far, the evolution) often appeared to be quite different. We analyzed literature data on aperture photometry and assembled a list of early-type galaxies whose nuclei are significantly redder than the bulges (Sil'chenko 1994), suggesting that these are candidates to have chemically distinct nuclei; the number of such candidates reached 25%–30% of the S0 galaxies considered. Subsequent two-dimensional spectroscopy of this sample has confirmed that, indeed, most of them have chemically distinct nuclei that are more metal rich by a factor of 2–10 than their nearest outskirts. However, curiously, these chemically distinct, metal-rich stellar nuclei, although redder, also appear to be younger than the bulges: for example, the mean luminosity-weighted stellar age in the nucleus in NGC 1023 is 7 Gyr, and in the nucleus in NGC 7332 as low as 2 Gyr, although their bulges have stellar populations as old as 15 Gyr (Sil'chenko 1999). Therefore, the red color in this case is a signature of a high mean metallicity and not of the homogeneously old age of the stars. On the other hand, among the lenticular galaxies with strong Balmer absorption lines in the integrated central-region spectra, there have been a few with rather *blue* nuclei. A natural question is: What is the difference between stellar populations in the red and blue nuclei of lenticular galaxies? Are the blue ones bluer due to lower age or due to lower metallicity, and do any differences in stellar population properties exist between the blue nuclei and their surrounding bulges? As a preliminary step toward answering these questions, we investigate here two intermediate-luminosity S0 galaxies with blue nuclei, NGC 5574 and NGC 7457. The global parameters of the galaxies are given in Table 1.

NGC 5574 is a close neighbor of the intermediate-luminosity elliptical NGC 5576 (with a separation of about of 20 kpc); the pair as a whole is detected in the 21 cm line (Lake & Schommer 1984), but no emission lines in the optical spectral range are seen, so no present star formation is suspected. In addition, when we studied the central part of

[1] Partly based on observations collected with the 6 m Bolshoi Teleskop Azimutal'nij at the Special Astrophysical Observatory of the Russian Academy of Sciences.

[2] Guest investigator of the UK Astronomy Data Centre.

TABLE 1
GLOBAL PARAMETERS OF THE GALAXIES

Parameter	Database	NGC 5574	NGC 7457
Type	NED	SBO–?sp	SA(rs)0–?
R_{25} (kpc)	LEDA	5.0	7.4
B_T^0	RC3	13.19	11.76
M_B	LEDA	−18.5	−18.6
$(B-V)_T^0$	RC3	0.82	0.83
$(U-B)_T^0$	RC3	0.31	0.32
V_r (km s^{-1})	NED	1659	812
Distance: $H_0 = 75$ km s^{-1} Mpc^{-1} (Mpc)	LEDA	23	12.2
Inclination (deg)	LEDA	59	70
PA_{phot} (deg)	LEDA	63	130

NGC 5576, we found a chemically distinct nucleus of a rather low age: the luminosity-weighted mean stellar age in the nucleus of NGC 5576 was found to be 3 Gyr, and a marginal iron overabundance was also detected (Sil'chenko 1997). Since faint outer stellar spiral arms are seen in NGC 5574 (Michard & Marchal 1994), one has to conclude that there is an interaction between the two galaxies that may affect the evolution of their central parts. We obtained multiaperture photoelectric data for NGC 5574 and measured the same $B-V$ colors in the nucleus and in the bulge ($\approx$0.8). Both of these are rather blue for an intermediate-luminosity lenticular (Sil'chenko 1989). Spectral investigation (Sil'chenko & Shapovalova 1989) has revealed strong Balmer absorption lines up to Hδ in the central region of the galaxy, so we are already prepared to find a young nucleus in NGC 5574, but the question of the bulge properties and also that of the circumnuclear disk signatures remain to be considered.

NGC 7457 is a visibly well-studied nearby lenticular galaxy. In particular, its surface photometry has been analyzed more than once, and Kormendy (1977) has cited its surface brightness profile as prototypical for an S0 galaxy. However, detailed consideration reveals some peculiarities even here. For example, the galaxy is known as disk-dominated, e.g., $D/B = 1.6$ is given by Burstein (1979), but Andredakis, Peletier, & Balcells (1995), who have fitted galactic bulges by Sersic's law with a free power $1/n$ and have claimed the existence of a correlation between relative bulge luminosity and n, have found an exclusive value of $n = 6$ for the bulge of NGC 7457, which is even steeper than the profiles of pure ellipticals. Peletier et al. (1999), from multiband photometry, have concluded that the bulge of NGC 7457 is unusually blue for its luminosity and that its colors imply a mean age of about 7 Gyr, whereas all the other bulges of their sample galaxies are about 10 Gyr old. To complete the picture of the peculiarities in the "prototypical S0 galaxy" NGC 7457, we must mention that although the galaxy lacks any emission lines, particularly in the nucleus (Ho, Filippenko, & Sargent 1995), and any detectable H I (Chamaraux, Balkowski, & Fontanelli 1987), a rather large amount of molecular gas is detected that is concentrated in the compact circumnuclear disk with a scale length much shorter than that of the global stellar disk (Taniguchi et al. 1994).

The layout of the paper is as follows. We report our observations and other data that we use in § 2. The radial variations of the stellar population properties are analyzed in § 3, and in § 4 two-dimensional stellar velocity fields obtained by integral-field spectroscopy are presented. Section 5 gives the discussion and our conclusions.

2. OBSERVATIONS AND DATA REDUCTION

The spectral data that we analyze in this work were obtained with two different integral-field spectrographs. Integral-field spectroscopy is a rather new approach that was first proposed by Professor G. Courtes some 15 years ago; for a description of the instrumental idea, see, e.g., Bacon et al. (1995). It allows us to simultaneously obtain a set of spectra in a wide spectral range from an extended area on the sky, for example, from the central part of a galaxy. A two-dimensional array of microlenses provides a set of micropupils that are put onto the entry of a spectrograph, and having reduced the full set of spectra corresponding to the individual spatial elements, we obtain a list of fluxes in continuum and in emission lines, of line-of-sight velocities for both stars and ionized gas, and of absorption-line equivalent widths, which are usually expressed as indices in the well-formulated Lick system (Worthey et al. 1994). This list can be transformed into two-dimensional maps of the above mentioned characteristics for the central part of the galaxy that is studied. Besides the panoramic view benefits, such an approach gives a unique opportunity to superpose various two-dimensional distributions over each other without any difficulties with positioning. In this work, we use the data in the green spectral range, 4200–5600 Å. These spectra are used to calculate the Lick indices Hβ, Mg b, Fe5270, and Fe5335, which are suitable for determining the mean stellar luminosity-weighted metallicity, age, and Mg/Fe ratio of old populations (Worthey 1994), and are also used for cross-correlation with spectra of template stars, usually of K0 III–K3 III spectral type, to obtain a line-of-sight velocity field for the stellar component and a map of stellar velocity dispersion. The list of the exposures made for NGC 5574 and NGC 7457 with two different two-dimensional spectrographs is given in Table 2.

The most recent variant of the Multipupil Fiber Spectrograph (MPFS) became operational in the prime focus of the 6 m Bolshoi Teleskop Azimutal'nij (BTA) in 1998.[3] Compared to the previous MPFS, in the new variant, the field of view is increased and the common spectral range is larger due to the use of fibers that transmit light from 16×15

[3] See http://www.sao.ru/~gafan/devices/mpfs/mpfs_main.htm.

TABLE 2
TWO-DIMENSIONAL SPECTROSCOPY OF NGC 5574 AND NGC 7457

Date	Galaxy	Exposure (minutes)	Configuration	Field (arcsec^2)	Spectral Range (Å)	Seeing (arcsec)
1999 Jun 6	NGC 5574	60	BTA/MPFS + CCD, 1024 × 1024	16 × 15	4200–5600	1.7
1999 Dec 13.....	NGC 7457	90	BTA/MPFS + CCD, 1024 × 1024	16 × 15	4200–5600	2.2
1999 Oct 11	NGC 7457 (1st position)	120	WHT/SAURON + CCD, 2k × 4k	33 × 41	4800–5400	1.8
	NGC 7457 (2st position)	60	WHT/SAURON + CCD, 2k × 4k	33 × 41	4800–5400	1.8
1999 Oct 12	NGC 7457 (2st position)	60	WHT/SAURON + CCD, 2k × 4k	33 × 41	4800–5400	1.1

square elements of the galaxy image to the slit of the spectrograph, together with an additional 16 fibers that transmit the sky background light, taken separately from the galaxy, so that separate sky exposures are not necessary. The size of one spatial element is approximately $1'' \times 1''$; a CCD TK 1024×1024 detector is used. The reciprocal dispersion is 1.35 Å per pixel, with a rather stable spectral resolution of 5 Å. To calibrate the wavelength scale, we use separate exposures of a helium, neon, and argon hollow cathode lamp; the internal accuracy of the fit to these calibration spectra is typically 0.25 Å in the green. In addition, we measured the [O I] λ5577 night sky emission line to check the accuracy of our calibration and found no systematic velocity shift. To calibrate the new MPFS index system onto the standard Lick one, we observed 15 stars from the list of Worthey et al. (1994) during four observational runs and calculated the linear regression formulae to transform our index measurements into the Lick system; the rms scatters of points near the linear dependencies are about 0.2 Å for all four indices under consideration, thus being within the observational errors of Worthey et al. (1994). To correct the index measurements for the stellar velocity dispersion, which is usually substantially nonzero in the centers of early-type galaxies, we have smoothed the spectrum of the standard star HD 97907 by a set of Gaussians of various widths; the derived dependencies of index corrections on σ were approximated by fourth-order polynomials and applied to the measured index values before their calibrations into the Lick system. However, in both galaxies considered here, the stellar velocity dispersion is below 100 km s^{-1}, so the correction for it is negligible.

The second two-dimensional spectrograph, the data of which we use in this work, is a new instrument operated at the 4.2 m William Herschel Telescope (WHT) on La Palma named SAURON; for its detailed description, see Bacon et al. (2001). We have taken the data for NGC 7457 obtained with it in 1999 October from the open Isaac Newton Group (ING) Archive of the UK Astronomy Data Centre.[4] The field of view of this instrument is $41'' \times 33''$, with a spatial element size of $0''.94 \times 0''.94$. The sky background $2'$ from the center of the galaxy was exposed simultaneously with the target. The spectral range is 4800–5400 Å, and the reciprocal dispersion is 1.11–1.21 Å varying from the left to the right edge of the frame. The comparison spectrum is a neon arc, and the linearization is made using a second-order polynomial fit with an accuracy of 0.07 Å. The index system is checked by using 12 stars from the list of Worthey et al. (1994) that were observed during the same observational run. Linear regressions were fitted to the dependence of the instrumental indices on the standard Lick indices (the rms scatters of the points about the fitting lines were below 0.2 Å, as in the case of the MPFS data), and these fits were used to transform our measurements into the standard Lick system.

The exposure times for the galaxies observed with the MPFS were chosen to be long enough to provide signal-to-noise ratios of more than 60 (per angstrom) in the nucleus and ~30 near the edges of the frames; the statistical error estimations made in the manner of Cardiel et al. (1998) range from 0.1 Å for NGC 7457 and 0.2 Å for NGC 5574 in the center to, correspondingly, 0.3 and 0.7 Å for the individual spatial elements in the outer parts. Besides constructing two-dimensional maps of indices, in order to obtain a constant level of accuracy along the radius, we co-added elementary spectra obtained with every two-dimensional spectrograph in concentric rings centered onto the nuclei and studied the radial dependencies of the stellar population properties by comparing the azimuthally averaged observed absorption-line indices with evolutionary synthesis models of old stellar populations by Worthey (1994). We estimate the typical accuracy of our azimuthally averaged indices as better than 0.1 Å.

In addition to the two-dimensional spectral data, we have obtained near-infrared (NIR) photometric data for the galaxies under consideration. The observations were made at the 2.1 m telescope of the National Astronomical Observatory of Mexico at San Pedro Martir, with the infrared camera CAMILA. The camera is equipped with the detector NICMOS 3, with a format of 256×256 pixels; a mode with a scale of $0''.85$ ($f/4.5$) was used. The details of the photometric observations are given in Table 3. Also, for NGC 7457 we have retrieved the NICMOS *Hubble Space Telescope* (*HST*) data from the *HST* Archive (program ID 7450, PI R. F. Peletier). The galaxy was observed on 1997 July 6 with the NIC 2 camera, through the filters F110W and F160W for 128 s each.

All the data, spectral and photometric, except the data obtained with the MPFS, were reduced with the software produced by V. V. Vlasyuk in the Special Astrophysical

TABLE 3
PHOTOMETRIC OBSERVATIONS OF NGC 5574 AND NGC 7457

Date	Galaxy	Filter	Exposure Time (minutes)	Seeing (arcsec)
2000 Mar 20	NGC 5574	*J*	8	3.5
	NGC 5574	*H*	6	2.9
	NGC 5574	*K'*	8	3.1
2001 Sep 7	NGC 7457	*J*	18	1.6
	NGC 7457	*H*	18	2.1

[4] See http://archive.ast.cam.ac.uk/ingarch.

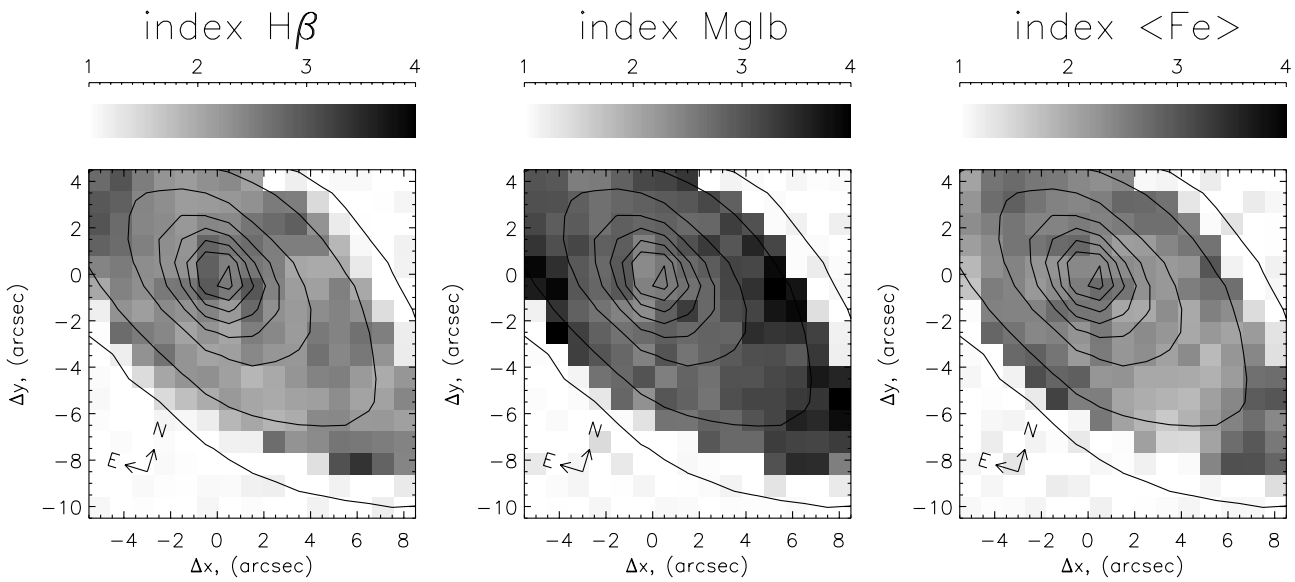

FIG. 1.—MPFS index maps for NGC 5574. A green (5000 Å) continuum is overlain by isophotes.

Observatory (Vlasyuk 1993). Primary reduction of the data obtained with the MPFS was done in IDL with software created by one of the authors (V. L. A.). The Lick indices were calculated with our own FORTRAN program as well as by using the FORTRAN program of A. Vazdekis.

3. STELLAR POPULATIONS IN THE CENTRAL REGIONS

3.1. *NGC 5574*

Figure 1 presents maps of the Lick indices Hβ, Mg b, and $\langle \mathrm{Fe} \rangle \equiv (\mathrm{Fe5270} + \mathrm{Fe5335})/2$ for the central part of NGC 5574. They are smoothed by a two-dimensional Gaussian with FWHM $= 2\farcs4$, except for the central $4'' \times 4''$. Since we knew about homogeneous color distribution in this object, we did not expect to see a chemically distinct nucleus. However, although the whole index distribution looks rather flat, the compact nucleus is somewhat outstanding. The iron index has a maximum near the center, and this feature is rather common, but the magnesium index shows a "hole," or a shallow minimum, in the very nucleus, which is quite unusual. One can say that an iron-overabundant nucleus is detectable "by eye." As usual, the hydrogen Hβ index qualitatively matches the $\langle \mathrm{Fe} \rangle$ distribution: it also demonstrates a maximum in the center. Thus, in the case of NGC 5574, we verify that the nucleus can be distinguished from the bulge by the properties of its stellar population and (by implication) by a different stellar evolutionary history.

Let us determine the characteristics of the stellar population in the center of NGC 5574 by comparing its Lick indices with those calculated for simple stellar population models by the evolutionary synthesis method. Figure 2 presents index-index diagrams in which we have plotted our azimuthally averaged measurements and the models of Worthey (1994). In the plot of Fe5270 versus Mg b, the models calculated in the frame of the solar chemical pattern $[\mathrm{Mg/Fe}] = 0$, except for various global metallicities and ages, occupy a narrow locus. The nucleus of NGC 5574 deviates significantly to the left of this locus, representing the rare phenomenon of an iron-overabundant stellar system. We note that most elliptical galaxies are magnesium overabundant and are located *to the right* of the model solar-ratio locus (Worthey, Faber, & Gonzalez 1992). The iron overabundance can sometimes be seen in irregular galaxies, and it is usually treated as a consequence of multiple discrete star formation bursts (Gilmore & Wyse 1991; Marconi, Matteucci, & Tosi 1994). Curiously, the nucleus of the neighboring elliptical galaxy NGC 5576 also seems to be iron overabundant (Sil'chenko 1997).

Age diagnostic diagrams commonly compare the hydrogen-line index, Hβ in our work, with one of the metal-line indices. In the case of NGC 5574, there are difficulties with the age determination in the nucleus, because the Worthey models are calculated for $[\mathrm{Mg/Fe}] = 0$ and the nucleus of the galaxy is iron overabundant. Comparing Hβ to Mg b or to $\langle \mathrm{Fe} \rangle$ (Fig. 2), we obtain slightly different estimates of the mean stellar age in the nucleus; however, the difference is not very large: 3 or 2 Gyr, respectively. In any case, it means that the nucleus of the lenticular galaxy NGC 5574 is rather young, or "poststarburst." Again, the mean age of the nuclear stellar population in NGC 5576 is also 3 Gyr (Sil'chenko 1997); are we dealing with synchronous multiple nuclear star formation bursts?

The bulge beyond $R \approx 2''$ has a solar magnesium-to-iron ratio, but it is also rather young: not older than 3–5 Gyr, with a global metallicity only slightly below the solar one. Therefore, we must conclude that the central bulge of NGC 5574 has also been polluted by recent star formation, not earlier than a few billion years ago.

3.2. *NGC 7457*

For this galaxy we have two sets of panoramic spectroscopic data that provide a unique opportunity to estimate the external accuracy of our results. Figure 3 presents maps of the Lick indices Hβ, Mg b, and $\langle \mathrm{Fe} \rangle \equiv (\mathrm{Fe5270} + \mathrm{Fe5335})/2$ obtained by using the MPFS data, and Figure 4 presents similar maps, except for the right panel, which is for Fe5270 only, obtained by using the SAURON data

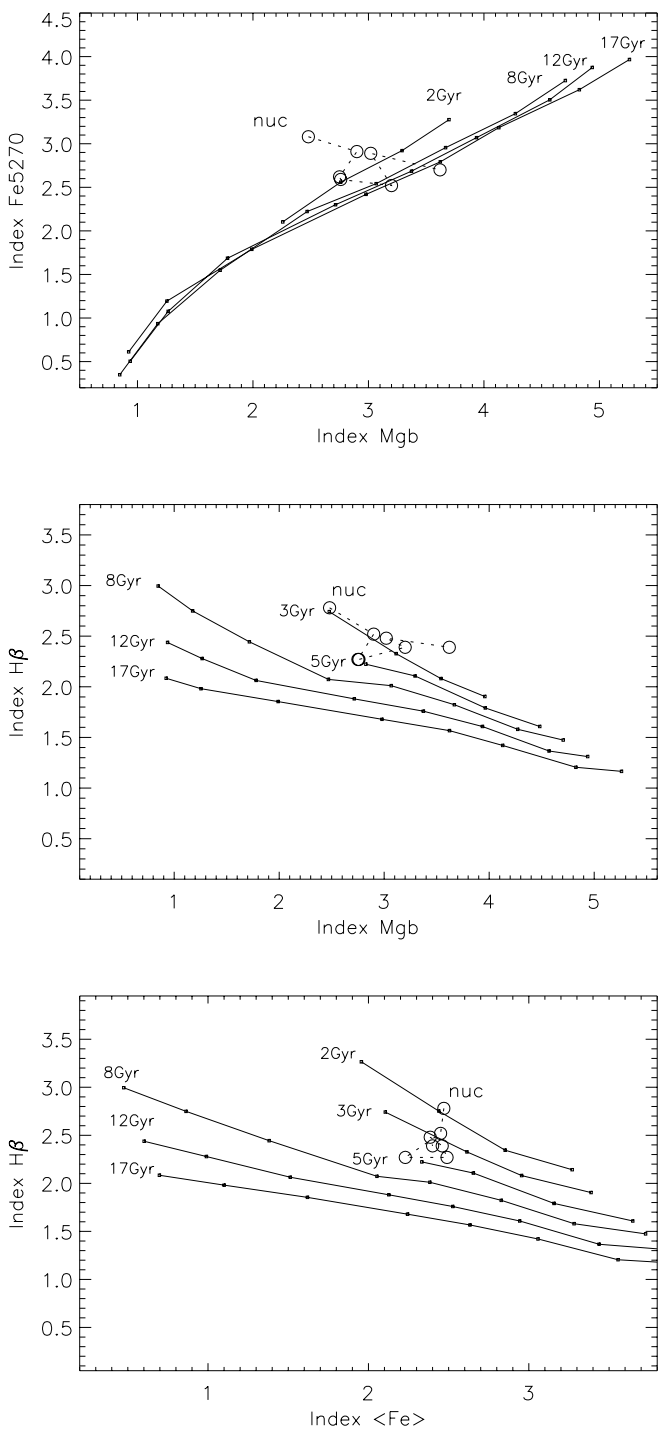

FIG. 2.—Index vs. index diagnostic diagrams for the azimuthally averaged index measurements in NGC 5574. The data points (*circles*) are taken along the radius of the galaxy with steps of 1″. As a reference, the model equal-age sequences from Worthey (1994) for old stellar populations with [Mg/Fe] = 0 are plotted by small squares connected with thin lines; the metallicities for the Worthey models are +0.50, +0.25, 0.00, −0.22, −0.50, −1.00, −1.50, and −2.00, if one follows the squares from right to left.

(more exactly, by using the first-position SAURON data, with the galaxy positioned closer to the frame bottom to avoid systematic distortion of Hβ at the frame top). We knew from our earlier MPFS observations that NGC 7457 did not possess a chemically distinct nucleus (Sil'chenko, Afanasiev, & Vlasyuk 1992). Indeed, the MPFS maps of all three indices (Fig. 3) obtained under a seeing of more than 2″ look very flat, with the nucleus quite indistinguishable against the bulge background. However, the SAURON maps (Fig. 4) obtained under seeing better than 2″ demonstrate marginal diffuse metal-index enhancements near the center and a quite definite Hβ-index maximum. We must admit that the nucleus of NGC 7457 is also distinct, but probably it is so faint and low-contrast that it can only be detected under rather good spatial resolution. The high signal-to-noise level of the SAURON data allows us to suggest that the region of the enhanced Hβ-index is elongated and extended roughly in the north-south direction, or close to the isophote minor axis. Let us note that the circumnuclear enhancement of the Hβ-index in NGC 5574 also looks extended (Fig. 1), but there the effect is seen near the limit of our spatial resolution.

To quantify the comparison of the MPFS and the SAURON Lick-index data, we plot together azimuthally averaged radial profiles of Hβ, Mg *b*, and Fe5270 measured from one MPFS and two SAURON data sets for two different nucleus positions on the frame (Fig. 5). In preparing the MPFS data, we co-added spectra in the rings; in preparing the SAURON data, which have the higher signal-to-noise ratios, we averaged the measured individual-element indices in the rings so that the attached error bars were the errors of the means. One can see a good agreement of all three data sets except for Hβ at $R < 5''$; since the estimate for the center of NGC 7457 made by Trager et al. (1998) in the $2'' \times 4''$ aperture, $H\beta = 2.47 \pm 0.19$, supports the SAURON data and since the two independent SAURON data sets made for the two different nucleus positions on the lens frame are in agreement, we consider the SAURON data for Hβ as more exact.

To determine stellar population characteristics in the nucleus and in the bulge of NGC 7457, let us consider together the index-index diagrams of Fe5270 versus Mg *b* and Hβ versus Mg *b* (Fig. 6). If we take into account the rather young mean age of the central stellar population in NGC 7457, we can assure ourselves that both the nucleus and the bulge have a close-to-solar magnesium-to-iron ratio, and because of this, we can surely use the models of Worthey (1994) to determine mean stellar ages. From Figure 6 (*bottom*) one can see that the nucleus, and only the nucleus resolved by the SAURON, has a luminosity-weighted age of the stellar population of less than 3 Gyr; this "young region" is not pointlike but has a radius of some 2″. The metallicity of the nuclear stellar population is approximately solar. The points corresponding to the bulge, according to all three data sets, occupy a parameter-space area between 3 and 8 Gyr and indicate a mean metallicity of about half of solar. These values are consistent with the results of Peletier et al. (1999), which are based on the broadband colors $B-I$ and $I-H$ and on quite different stellar population models: they have obtained $T = 4$ Gyr and $Z \approx 0.02$ for the nucleus and $T = 7$ Gyr and $Z \approx 0.008$ for the bulge of NGC 7457. Curiously, such a combination of parameters forces the optical colors, $B-V$ in our previous analysis (Sil'chenko 1994) and $B-I$ in the measurements of Peletier et al. (1999), to be similar in the nucleus and in the bulge, but results in a prominent difference of the NIR color $I-H$. In general, the broadband optical colors are highly degenerative with respect to the effects of age and metallicity: an increase of each of these parameters results in a similar degree of reddening; for a quantitative model estimate of

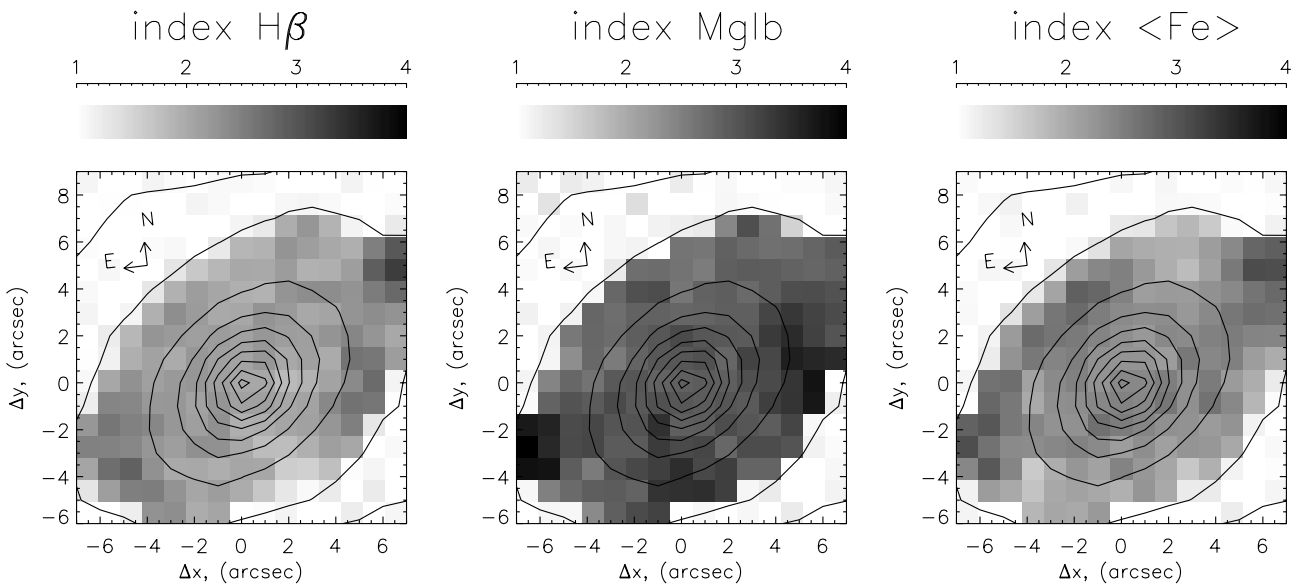

FIG. 3.—MPFS index maps for NGC 7457. A green (5000 Å) continuum is overlain by isophotes.

the degeneracy degree, see Worthey (1994). Even using two-color diagrams does not save the situation, because for example, on the diagram of ($U-B$, $B-V$), metal-poor old globular clusters and dwarf ellipticals occupy the same area as star-forming spiral galaxies with a solar metallicity (Zasov & Sil'chenko 1983; Sil'chenko 1985). This degeneracy may result in a situation when color gradients are absent in a galaxy but the properties of the stellar population, and some absorption-line indices, change along the radius. Just such a case can be found in the well-studied dE galaxy M32, in which the broadband colors are homogeneous but the indices Hβ, Fe5270, and Fe5335 demonstrate significant negative gradients, implying a younger and more metal-rich nucleus than the whole galaxy (Davidge 1991). Therefore, the same $V-I$ colors of the circumnuclear disks and of their surrounding spheroids found in the *HST*-based study of kinematically distinct nuclei in elliptical galaxies by Carollo et al. (1997) do not mean in fact similar stellar populations in the nucleus and in the total galaxy: the bluing due to younger age may be compensated by reddening due to higher metallicity. In the particular case of NGC 7457, we must reconsider the older diagnosis of Sil'chenko et al. (1992) and conclude that the nucleus of this galaxy is probably chemically distinct, with a metallicity difference of a factor of 2 between the nucleus and the bulge. However, in what is rather atypical for a lenticular galaxy with a chemically distinct nucleus, the bulge of NGC 7457 is rather young, with a mean age of the stellar population of 6–7 Gyr, although it is still older than the nucleus, which is less than 3-Gyr old.

4. STELLAR KINEMATICS IN THE CENTRAL REGIONS

Since the integral-field spectroscopy provides us with two-dimensional line-of-sight velocity fields, we are now

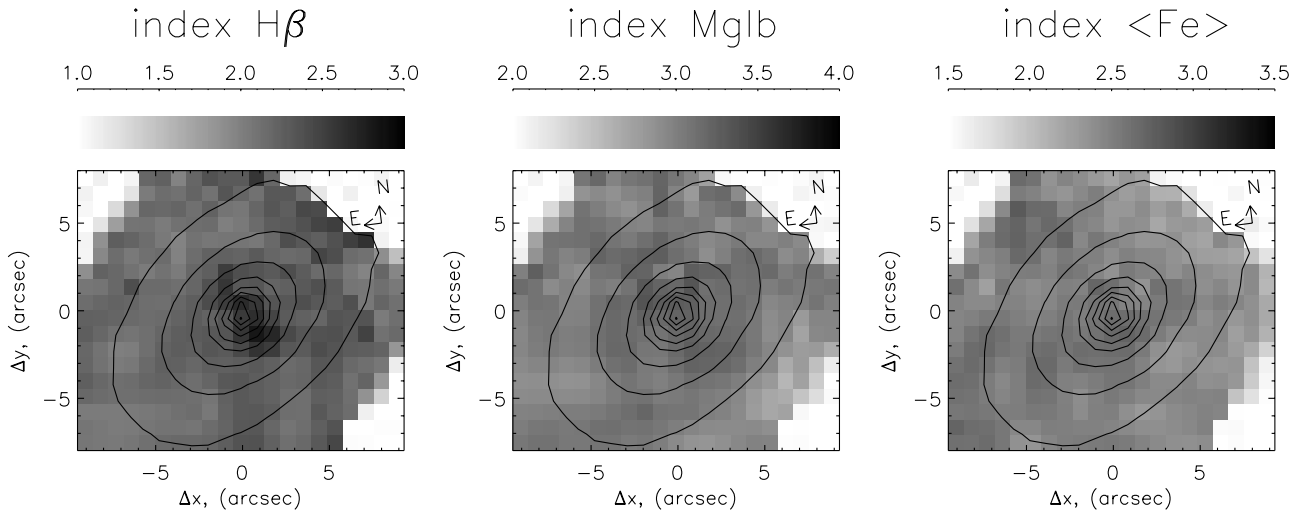

FIG. 4.—SAURON index maps for NGC 7457. A green (5000 Å) continuum is overlain by isophotes.

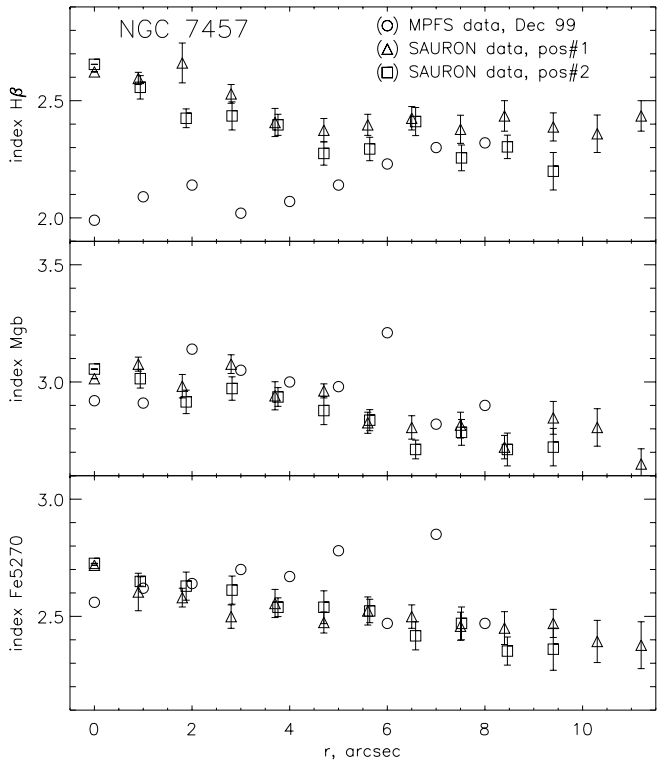

FIG. 5.—Comparison of two SAURON sets and one MPFS set of azimuthally averaged index measurements for NGC 7457. The MPFS spectra are co-added and the two-dimensional SAURON index measurements are azimuthally averaged in concentric rings centered on the nucleus.

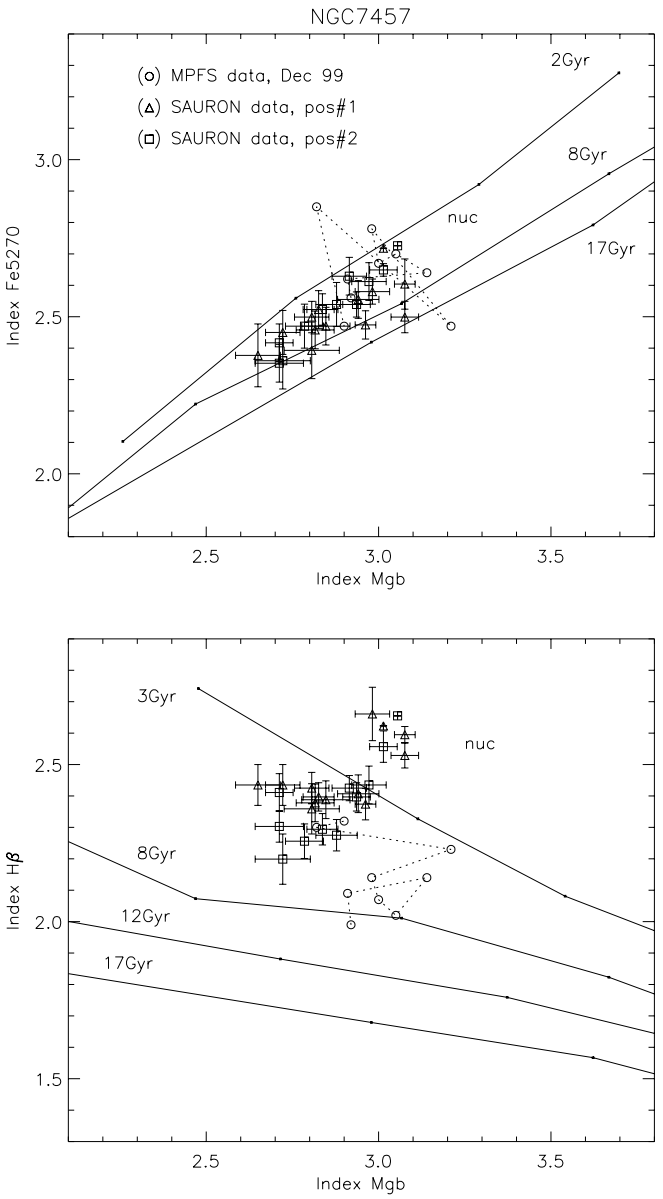

FIG. 6.—Index vs. index diagnostic diagrams for the azimuthally averaged index measurements in NGC 7457. The data points are taken along the radius of the galaxy with steps of 1″; the MPFS data points (*circles*) are connected by a dashed line in the direction of increasing radius, and the SAURON data for the bulge are given as a homogeneous point cloud (*triangles, open squares*), whereas the nucleus is marked by "nuc." As a reference, the model equal-age sequences from Worthey (1994) for old stellar populations with [Mg/Fe] = 0 are plotted by small filled squares connected with thin lines; the metallicities for the Worthey models are +0.50, +0.25, 0.00, and −0.22 for the 2 Gyr model, +0.25, 0.00, and −0.22 for the 3 Gyr model, 0.00, −0.22, and −0.50 for the 8 Gyr model, and −0.22 and −0.50 for the 12 Gyr and 17 Gyr models, respectively, if one follows the small filled squares from right to left.

able to analyze both the characteristics of the rotation and the degree of axisymmetry in the central structure components. If we have an axisymmetric mass distribution and rotation in circular orbits, the direction of the maximum central line-of-sight velocity gradient (we call it the "kinematical major axis") should coincide with the line of nodes as well as with the photometric major axis, whereas in the case of a triaxial potential, the isovelocities should align with the principal axis of the ellipsoid, and the kinematical and photometric major axes should generally diverge, showing turns with respect to the line of nodes in opposite directions (Monnet, Bacon, & Emsellem 1992; Moiseev & Mustsevoy 2000). In the simple case of cylindrical (disklike) rotation, we have a convenient analytical expression for the azimuthal dependence of central line-of-sight velocity gradients within the area of solid-body rotation: $dv_r/dr = \omega \sin i \cos(\mathrm{PA} - \mathrm{PA}_0)$, where ω is the deprojected central angular rotation velocity, i is the inclination of the rotation plane, and PA_0 is the orientation of the line of nodes, coinciding in the case of an axisymmetric ellipsoid (or a thin disk) with the photometric major axis. Therefore, by fitting azimuthal variations of the central line-of-sight velocity gradients with a cosine curve, we can determine the orientation of the kinematical major axis by its phase and the central angular rotation velocity by its amplitude. It is our main tool of kinematical analysis.

4.1. *NGC 5574*

Figure 7 shows the line-of-sight velocity field and the map of the velocity dispersion for the stellar component in the center of NGC 5574 according to our MPFS data. The stellar velocity field demonstrates a regular, quasi–solid-body rotation, with $\omega \sin i = 10 \pm 3$ km s^{-1} arcsec^{-1} at $R \leq 2''$ and 9 ± 4 km s^{-1} arcsec^{-1} at $R = 3''$–$5''$. The stellar velocity dispersion, being rather low over the whole field of view, reveals a flat maximum in the center, elongated along the major axis of the isophotes. To explain the kinematical properties of the galactic central region, we should compare the orientations of the kinematical and photometric structures.

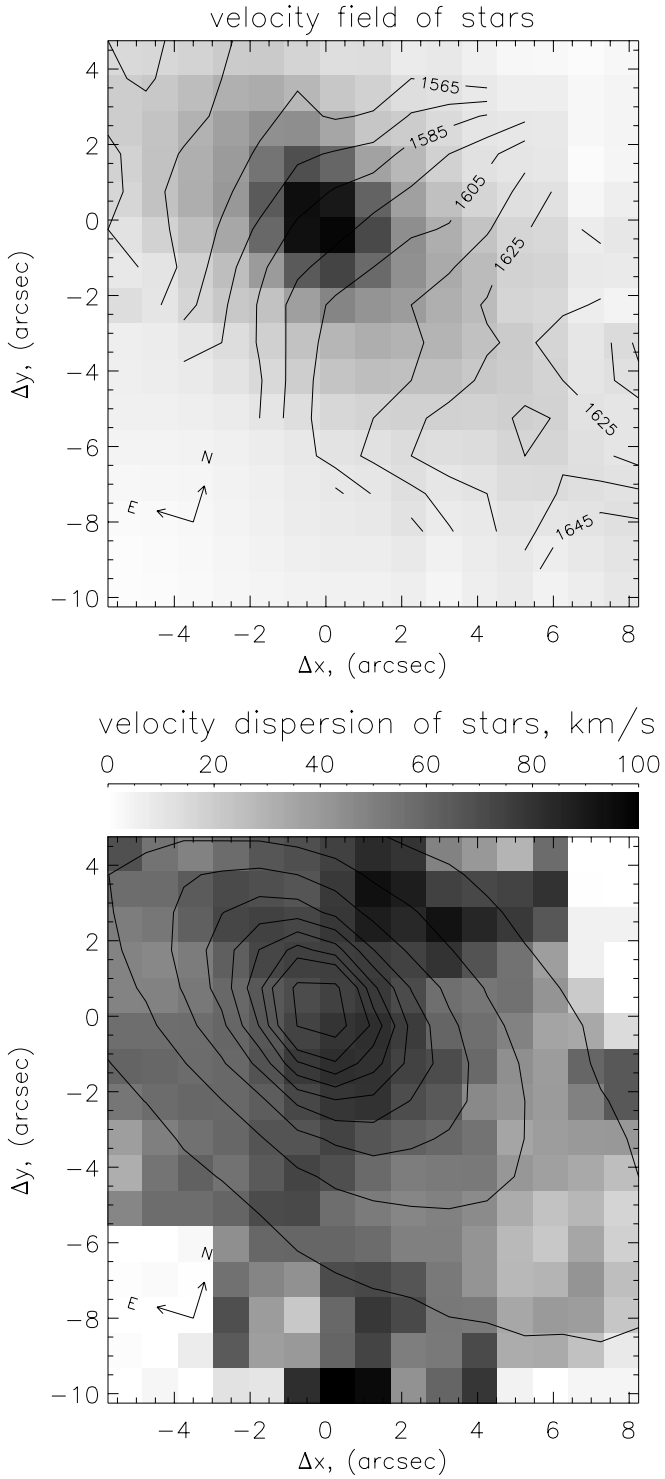

FIG. 7.—Line-of-sight velocity field for the stellar component (isolines superposed over the continuum image) and stellar velocity dispersion map (gray scale, with the green continuum isophotes superposed) in the center of NGC 5574.

To avoid problems with dust-effect uncertainty, in this work we use NIR photometric data. Figure 8 presents radial variations of the major-axis position angle measured from the *JHK* images obtained with CAMILA. For the outermost part, we check our measurements by using the Digitized Sky Survey (DSS) image of NGC 5574. Although diverging at $R < 5''$ because of bad seeing quality, all three photometric data sets reveal a slight turn of isophotes by some 5° in the inner part of the galaxy, at $R < 20''$; let us remember that NGC 5574 possesses a bar (see Table 1) aligned almost exactly with the line of nodes, and the kinematical major axis, determined by fitting azimuthal variations of the line-of-sight velocity gradients by a cosine law, also turns, but in the opposite sense: at $R \leq 3''.5$, we obtain in two radial bins a kinematical major axis of $PA_0 = 240°$, or 60° in Figure 8, which differs by 3° from the line-of-nodes orientation. Although the deviations by 3°–5° are close to the limit of our determination accuracy, the whole picture—the turns of the photometric and kinematical major axes by the same angle in the opposite sense with respect to the line of nodes—is quite consistent with the probable bar influence on the stellar kinematics in the center of the galaxy. Another feature that can be attributed to the bar influence is the lower than usual stellar velocity dispersion (for stellar velocity dispersion statistics in S0s, see Kormendy & Illingworth 1983) and its maximum area elongation along the bar direction: the latter effect has been theoretically predicted by Vauterin & Dejonghe (1997) and observationally demonstrated by Moiseev (2001).

4.2. *NGC 7457*

Concerning the whole picture of the stellar kinematics in the center of NGC 7457, we can compare our MPFS data with those from SAURON, but as for subtle details, the better spatial resolution of the SAURON data is crucial in revealing a much more complex dynamical structure of the galaxy than has been thought before. Figure 9 presents three different measurements of the stellar velocity field, one from MPFS and two from SAURON, with different nucleus positions on the frame, smoothed by a two-dimensional Gaussian with FWHM = 2″.35. All three pictures are quite consistent with each other: we observe large-scale quasi–solid-body rotation: rather slow, $\omega \sin i = (4.8 \pm 0.4)$ km s^{-1} arcsec^{-1}, but very regular. However, the small-scale pattern of the isovelocities is somewhat wavy, and in particular, both SAURON velocity maps, although being smoothed, nevertheless reveal a strange isovelocity turn in the very nucleus. An attentive examination of the central part of the unsmoothed kinematical maps (Fig. 10) gives an explanation for this disturbance: NGC 7457 has a counterrotating core. More exactly, the probable turn of the kinematical major axis in the center of the galaxy is about 130°–140°, but it is very difficult to measure it with more confidence because of the extreme compactness of the counterrotating component: its radius is less than 2″. For the two different positions of the nucleus on the lens array, we obtain $PA_0 = 152°$ for the kinematic axis of position 2, when the nucleus is within a single lens and the spatial resolution is the best, and $PA_0 = 185°$ for the kinematic axis of position 1, when the nucleus is between two neighboring lenses. The corresponding angular rotation velocity estimates are 16 ± 7 and 6 ± 4 km s^{-1} arcsec^{-1}; the former estimate, obtained under a seeing quality of 1″, implies a rather fast core rotation. Another interesting feature in Figure 10 related to the first one is a significant minimum of the stellar velocity dispersion in the nucleus of NGC 7457. An examination of the picture from the MPFS (Fig. 10 [*left*]) confirms the minimum of the stellar velocity dispersion in the nucleus. We think that in this particular case, the increase of the stellar velocity dispersion with the radius can be

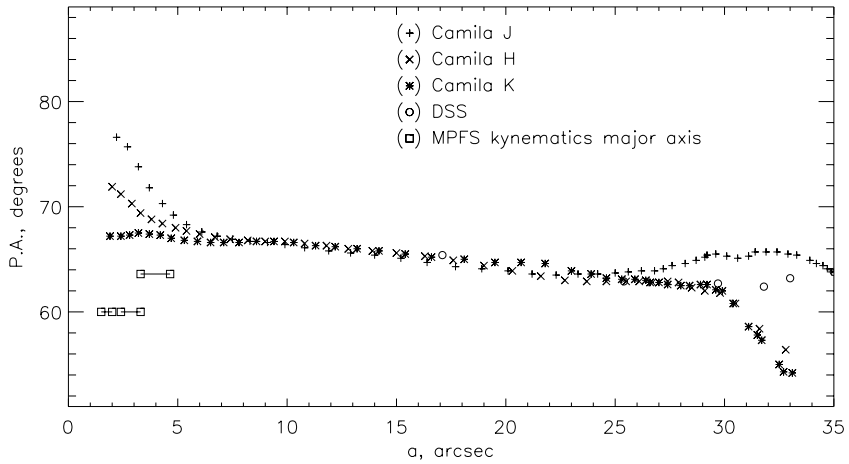

FIG. 8.—Comparison of the orientations of the isophote (photometric) major axis and the kinematical major axis (see the text) in NGC 5574

explained by a superposition of two quasi-counterrotating stellar subsystems. A very similar effect is observed in NGC 4550, a lenticular galaxy with well-known counterrotating large-scale cold stellar disks (Rix et al. 1992): when it was observed with a low spectral resolution, its central region seemed not to be rotating at all, with a small central velocity dispersion sharply rising along the radius. As for NGC 7457, here it would be even more difficult to separate counterrotating stellar subsystems than in NGC 4550, because NGC 7457 is not edge-on as NGC 4550 is, and the line-of-sight velocity separation of the components in it is smaller and therefore hardly measurable.

To check the validity of our velocity measurements in NGC 7457, we have simulated one-dimensional (e.g., long-slit) cross sections of the maps of Figures 9 and 10 at PA = 130° and have compared them with the published long-slit data of Simien & Prugniel (1997). In Figure 11 it is evident that the agreement is excellent for both the line-of-sight velocities and the stellar velocity dispersion measurements. Even some hints of the nonmonotonic behavior, which was clearly seen in the two-dimensional maps, can be seen here too, although an accuracy of 15 km s^{-1} for individual positions along the long slit in the data of Simien & Prugniel (1997) is quite insufficient to make conclusions based only on the one-dimensional data.

Finally, Figure 12 presents a comparison of the orientations of the photometric and kinematical major axes in the center of NGC 7457. Bearing in mind that the line of nodes of the galaxy is at PA = 126° (from our *JH* photometry for the outermost parts of the galaxy), one must admit that all the NIR photometry, both from the *HST* and ground-based, indicates strong geometrical distortions inside $R \approx 3''$. In the very center, $R < 1''$, isophotes turn in a positive sense, up to PA ≈ 160°, and farther from the nucleus, over a small radius range of 1″–2″, they turn in the negative sense, by some 6°–8° with respect to the line of nodes. Curiously, the radial variations of the kinematical major axis orientation repeat this trend exactly, but with some shift outward. Whether this shift is due only to lower spatial resolution (at least, with respect to the *HST* data) or whether there is a physical reason for such a relation between the photometric and kinematical characteristics cannot be answered in this work. However, we can surely state that the "counterrotating" stellar subsystem in the center of NGC

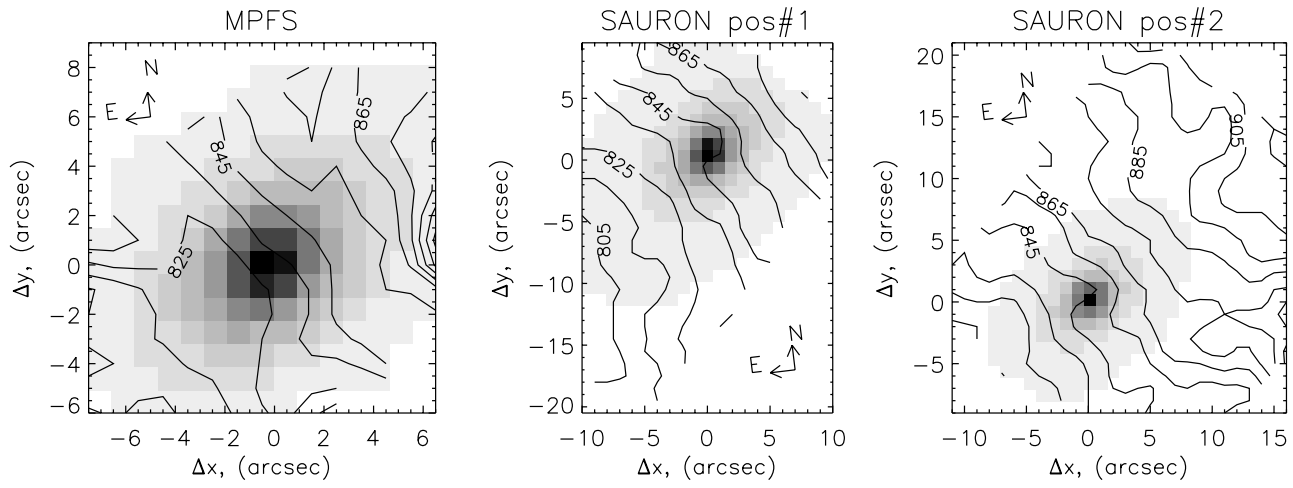

FIG. 9.—Line-of-sight velocity fields for the stellar component (isolines superposed over the continuum image) in the center of NGC 7457 according to MPFS data and to two data sets from SAURON. The maps are smoothed by a two-dimensional Gaussian with $\sigma_{x,y} = 1''$.

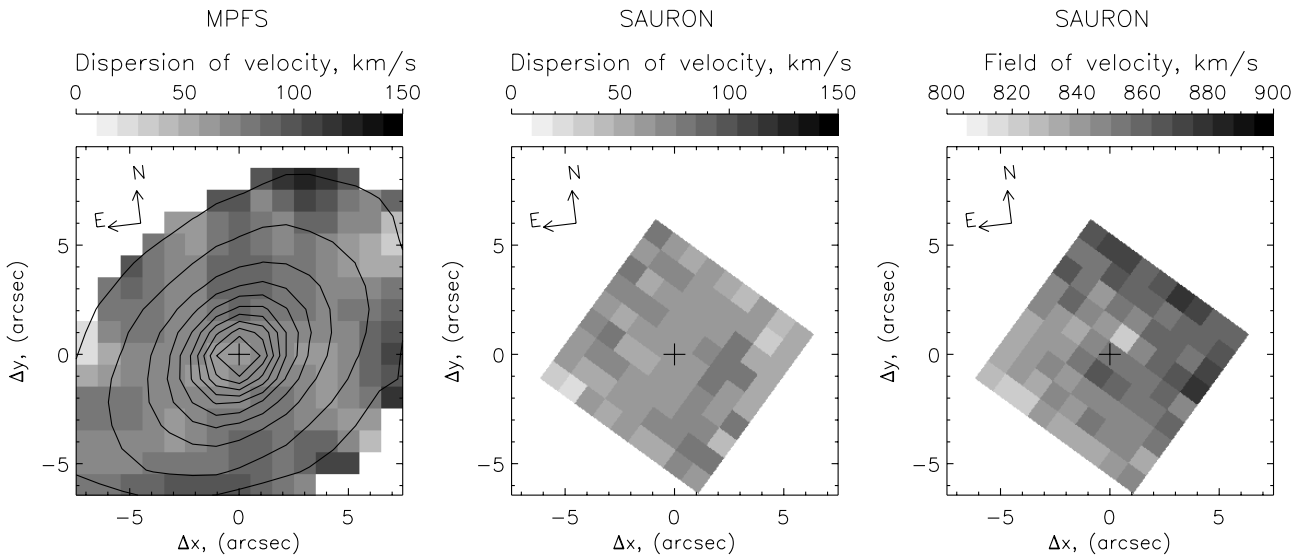

FIG. 10.—Unsmoothed kinematic maps for the center of NGC 7457. *Left*: Velocity dispersion measurements from MPFS. *Middle*: Velocity dispersion measurements from SAURON, position 2. *Right*: Stellar line-of-sight velocity field from SAURON, position 2. The cross marks the photometric center.

7457 rotates axisymmetrically, although its rotation plane is inclined with respect to the global symmetry plane of the galaxy.

5. CONCLUSIONS AND DISCUSSION

We have studied the stellar populations in the centers of two lenticular galaxies previously known to have radially homogeneous blue optical-band colors: NGC 5574 and NGC 7457. Despite our expectations, the compact nuclei of the galaxies appear to be chemically distinct: in NGC 5574 the nucleus is distinguished by a higher than solar iron-to-magnesium ratio, and in NGC 7457 a drop of the global metallicity by a factor of 2 exists between the nucleus and the bulge. An unusual (at least, as far as we know yet) property of both galaxies is a rather young mean stellar luminosity-weighted age of the stellar populations in their bulges, not older than 5–7 Gyr, but the chemically distinct nuclei are still younger, 2–2.5 Gyr old. The kinematics of the stars in the center of NGC 5574 are probably responsive to the influence of its global bar. The compact core of NGC 7457, with a radius of about 1″.5, demonstrates a visible counterrotation; a combined analysis of the photometric and kinematical two-dimensional maps allows us to conclude that this core rotates axisymmetrically, but its rotation plane is inclined to the main symmetry plane of the galaxy. The stellar velocity dispersion in the centers of both galaxies is anomalously low: 60–80 km s^{-1}.

Of the two galaxies under consideration, NGC 7457 has been much more intensively studied than NGC 5574. Now, with our new understanding of the central structure of NGC 7457, we can comment on some long-standing puzzles related to this galaxy. As we mention above, NGC 7457 has an unusually low measured central velocity dispersion: ~60 km s^{-1} in the very nucleus and 80–90 km s^{-1} to the north and to the south of the nucleus. This fact was noted for the first time by Kormendy & Illingworth (1983), who tried to derive an L versus σ_0 relation for the bulges of S0–Sbc galaxies. Among the 25 SA0–SAbc galaxies of their sample, 23

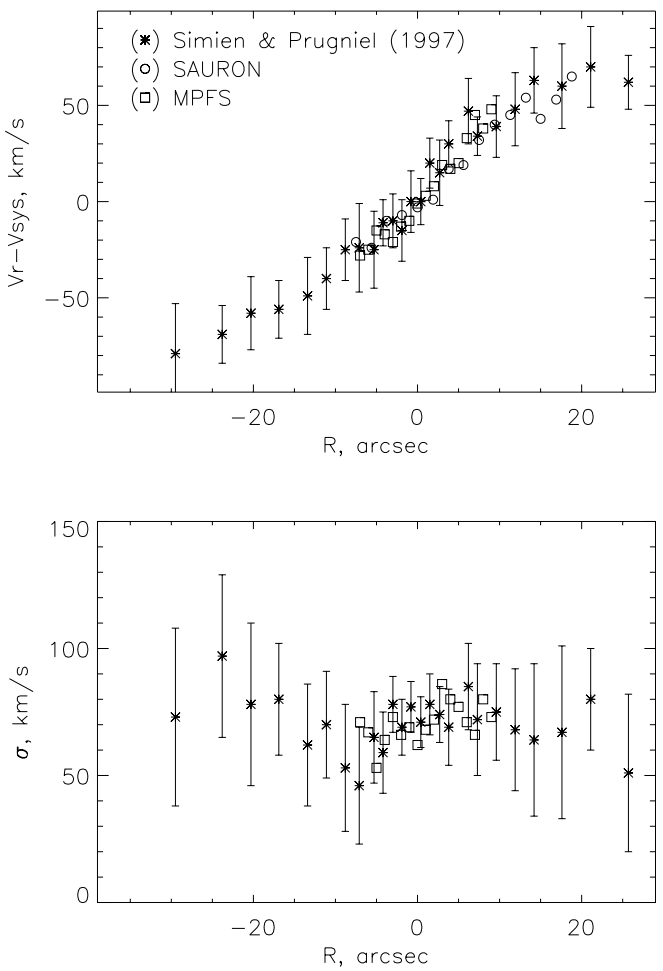

FIG. 11.—Comparison of the simulated one-dimensional cross sections at PA = 130° of our kinematic maps for NGC 7457 with the published long-slit data of Simien & Prugniel (1997). *Top*: Relative stellar line-of-sight velocity. *Bottom*: Stellar velocity dispersion.

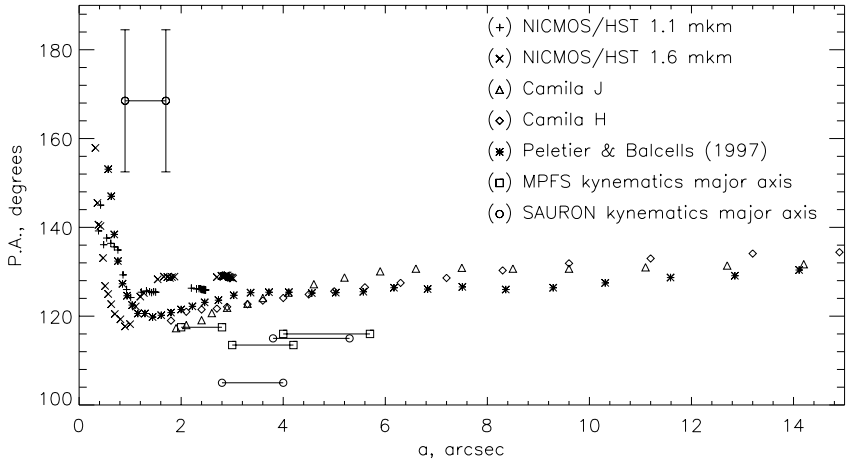

FIG. 12.—Comparison of the orientations of the isophote (photometric) major axis and the kinematical major axis (see the text) in NGC 7457. Besides our data, the results of *K*-photometry by peletier & Balcell (1997) are also plotted.

obeyed a very tight relation, $L \propto \sigma_0^{7.8}$, and only two, including NGC 7457, were strongly off; the gap between NGC 7457 and the main cloud of points was twice as large as the scatter around the relation. The authors could not explain this anomaly. The same year, Dressler & Sandage (1983) studied the *rotation* of lenticular galaxies. Again, NGC 7457 appeared to fall off the mean relation between luminosities and rotation velocities for the lenticular galaxies: its formal estimate of M/L made from the measured $v_{\max}$ and M_B (from the Tully-Fisher diagram) was found to be about 1, less than the mean for Sc galaxies. The authors thought it to be improbable and concluded that since "the observed rotation value for galaxies such as NGC 7457... is not sufficient to account for the masses of these galaxies," these galaxies, including NGC 7457, were supported by "internal velocity dispersions." However, Kormendy & Illingworth (1983) had just found that the velocity dispersion of NGC 7457 is too low for its luminosity! This raises the question: Where is the kinetic energy of the galaxy? The observations reported here suggest not one, but two solutions for this problem. The first solution is based on an analogy with NGC 4550. NGC 4550 was also thought to be nonrotating, with a central velocity dispersion of 86 ± 7 km s^{-1} (Tonry & Davis 1981), until two counterrotating stellar disks were found in this galaxy (Rubin, Graham, & Kenney 1992; Rix et al. 1992). Since now we know that NGC 7457 has a counterrotating core, we can suggest that some part of the stars at larger radii may counterrotate too, visibly diminishing the rotation velocity obtained from the spectra integrated along the line of sight. The second possibility is that because the bulge stellar population in NGC 7457 is significantly younger than stellar populations in most other bulges (Peletier et al. 1999), it must really demonstrate a lower M/L_B than the bulk of other lenticulars. The two effects together may perhaps explain the unusual kinematics of the galaxy.

However, whereas these previous puzzles are probably solved, new puzzles arise. The bulges in NGC 5574 and NGC 7457 have rather young stellar populations. A natural conclusion is that they have been recently formed by secular evolution. Indeed, NGC 5574 has a well-known bar; in § 4 we have seen that the central stellar kinematics of the galaxy support the dynamical importance of the bar in this galaxy. NGC 7457, although classified as SA0, is also not completely axisymmetric: it demonstrates variations of the isophote major axis position angle, and Michard & Marchal (1994) have noted the possible presence of a bar in this galaxy. Both galaxies possess some gas: H I is detected in NGC 5574 (Haynes et al. 1997) and CO in NGC 7457 (Taniguchi et al. 1994). Thus, there is material for the secular evolution of the bulges, there is a mechanism for inducing circumnuclear star formation, and consequently, such evolution is highly probable. However, a common view is that secular evolution produces exponential-profile bulges (see, e.g., Courteau, de Jong, & Broeils 1996, and references therein), and both NGC 5574 and NGC 7457 possess classical de Vaucouleurs profiles. For NGC 7457, it has been established more than once, starting from the photographic photometry of Burstein (1979), and for NGC 5574, there is a nice bulge-disk decomposition by Baggett, Baggett, & Anderson (1998). We ourselves have checked this with our photometric data; indeed, the de Vaucouleurs' law is the best for their bulges. On the other hand, Aguerri, Balcells, & Peletier (2001) have argued that a de Vaucouleurs profile of a bulge can only be the product of a dense satellite merger. These considerations thus raise a new possibility: our data for NGC 5574 and NGC 7457 may provide the first direct evidence for merger-driven evolution in disk galaxies.

We thank S. N. Dodonov and the postgraduate student of the Special Astrophysical Observatory A. V. Moiseev for supporting the observations at the 6 m telescope. The 6 m telescope is operated under the financial support of the Science Ministry of Russia (registration number 01-43); we also thank the Programme Committee of the 6 m telescope for allocating observational time. During the data analysis, we used the Lyon-Meudon Extragalactic Database (LEDA) supplied by the LEDA team at the CRAL-Observatoire de Lyon (France) and the NASA/IPAC Extragalactic Database (NED), which is operated by the Jet Propulsion Laboratory, California Institute of Technology, under contract with the National Aeronautics and Space Administration. The work is partially based on data taken from the ING

Archive of the UK Astronomy Data Centre and on observations made with the NASA/ESA *HST*, obtained from the data archive at the Space Telescope Science Institute. STScI is operated by the Association of Universities for Research in Astronomy, Inc., under NASA contract NAS 5-26555. The study of the young nuclei in lenticular galaxies is supported by the grant of the Russian Foundation for Basic Researches 01-02-16767 and by the Federal Scientific-Technical Program contract of the Science Ministry of Russia 40.022.1.1.1101.

REFERENCES

Aguerri, J. A. L., Balcells, M., & Peletier, R. F. 2001, A&A, 367, 428
Andredakis, Y. C., Peletier, R. F., & Balcells, M. 1995, MNRAS, 275, 874
Bacon, R., et al. 1995, A&AS, 113, 347
———. 2001, MNRAS, 326, 23
Baggett, W. E., Baggett, S. M., & Anderson, K. S. J. 1998, AJ, 116, 1626
Burstein, D. 1979, ApJ, 234, 435
Buta, R., & Williams, K. L. 1995, AJ, 109, 543
Cardiel, N., Gorgas, J., Cenarro, J., & Gonzalez, J. J. 1998, A&AS, 127, 597
Carollo, C. M., Franx, M., Illingworth, G. D., & Forbes, D. A. 1997, ApJ, 481, 710
Chamaraux, P., Balkowski, C., & Fontanelli, P. 1987, A&AS, 69, 263
Courteau, S., de Jong, R. S., & Broeils, A. H. 1996, ApJ, 457, L73
Davidge, T. J. 1991, AJ, 101, 884
Dressler, A., & Sandage, A. 1983, ApJ, 265, 664
Gilmore, G., & Wyse, R. F. G. 1991, ApJ, 367, L55
Haynes, M. P., Giovanelli, R., Herter, T., Vogt, N. P., Freudling, W., Maia, M. A. G., Salzer, J. J., & Wegner, G. 1997, AJ, 113, 1197
Ho, L. C., Filippenko, A., & Sargent, W. L. 1995, ApJS, 98, 477
Kormendy, J. 1977, ApJ, 214, 359
Kormendy, J., & Illingworth, G. 1983, ApJ, 265, 632
Lake, G., & Schommer, R. A. 1984, ApJ, 280, 107
Marconi, G., Matteucci, F., & Tosi, M. 1994, MNRAS, 270, 35
Michard, R., & Marchal, J. 1994, A&AS, 105, 481
Moiseev, A. V. 2001, Bull. Spec. Astrophys. Obs., 51, 140
Moiseev, A. V., & Mustsevoy, V. V. 2000, Pis'ma v AZh., 26, 657
Monnet, G., Bacon, R., & Emsellem, E. 1992, A&A, 253, 366
Peletier, R. F., & Balcells, M. 1997, NewA, 1, 349
Peletier, R. F., Balcells, M., Davies, R. L., Andredakis, Y., Vazdekis, A., Burkert, A., & Prada, F. 1999, MNRAS, 310, 703
Rix, H.-W., Franx, M., Fisher, D., & Illingworth, G. 1992, ApJ, 400, L5
Rubin, V. C., Graham, J. A., & Kenney, J. D. P. 1992, ApJ, 394, L9
Sil'chenko, O. K. 1985, Ap&SS, 117, 83
———. 1989, Pis'ma v AZh., 15, 493
———. 1990, Soob. Spec. Astrophys. Obs., 65, 75
———. 1993, Pis'ma v AZh., 19, 693
———. 1994, AZh, 71, 706
———. 1997, AZh, 74, 643
———. 1999, AJ, 117, 2725
Sil'chenko, O. K., Afanasiev, V. L., & Vlasyuk, V. V. 1992, AZh, 69, 1121
Sil'chenko, O. K., & Shapovalova, A. I. 1989, Soob. Spec. Astrophys. Obs., 60, 44
Simien, F., & Prugniel, Ph. 1997, A&AS, 126, 519
Taniguchi, Y., Murayama, T., Nakai, N., Suzuki, M., & Kameya, O. 1994, AJ, 108, 468
Tonry, J. L., & Davis, M. 1981, ApJ, 246, 666
Trager, S. C., Worthey, G., Faber, S. M., Burstein, D., & Gonzalez, J. J. 1998, ApJS, 116, 1
Vauterin, P., & Dejonghe, H. 1997, MNRAS, 286, 812
Vlasyuk, V. V. 1993, Astrofiz. Issled. (Izv. SAO RAS), 36, 107
Worthey, G. 1994, ApJS, 95, 107
Worthey, G., Faber, S. M., & Gonzalez, J. J. 1992, ApJ, 398, 69
Worthey, G., Faber, S. M., Gonzalez, J. J., & Burstein, D. 1994, ApJS, 94, 687
Zasov, A. V., & Sil'chenko, O. K. 1983, AZh, 60, 1063